Available online at www.sciencedirect.com
SCIENCE DIRECT®
Biology of the Cell 96 (2004) 701–711
Biology of the Cell
www.elsevier.com/locate/biocell

TPPP/p25: from unfolded protein to misfolding disease: prediction and experiments

F. Orosz [a,1], G.G. Kovács [b,1], A. Lehotzky [a], J. Oláh [a], O. Vincze [a], J. Ovádi [a,*]

[a] *Institute of Enzymology, Biological Research Centre, Hungarian Academy of Sciences, Karolina út 29, 1113 Budapest, Hungary*
[b] *National Institute of Psychiatry and Neurology, Hűvösvölgyi út 116, 1021 Budapest, Hungary*

Received 28 May 2004; accepted 12 August 2004

Available online 07 October 2004

Abstract

TPPP/p25, the first representative of a new protein family, identified as a brain-specific unfolded protein induces aberrant microtubule assemblies in vitro, suppresses mitosis in *Drosophila* embryo and is accumulated in inclusion bodies of human pathological brain tissues. In this paper, we present prediction and additional experimental data that validate TPPP/p25 to be a new member of the "intrinsically unstructured" protein family. The comparison of these characteristics with that of α-synuclein and tau, involved also in neurodegenerative diseases, suggested that although the primary sequences of these proteins are entirely different, there are similarities in their well-defined unstructured segments interrupted by "stabilization centres", phosphorylation and tubulin binding motives. SK-N-MC neuroblastoma cells were transfected with pEGFP-TPPP/p25 construct and a stable clone denoted K4 was selected and used to establish the effect of this unstructured protein on the energy state/metabolism of the cells. Our data by analyzing the mitochondrial membrane polarization by fluorescence microscopy revealed that the high-energy phosphate production in K4 clone is not damaged by the TPPP/p25 expression. Biochemical analysis with cell homogenates provided quantitative data that the ATP level increased 1.5-fold and the activities of hexokinase, glucosephosphate isomerase, phosphofructokinase, triosephosphate isomerase and glyceraldehyde-3-phosphate dehydrogenase were 1.2 to 2.0-fold higher in K4 as compared to the control. Our modelling using these data and rate equations of the individual enzymes suggests that the TPPP/p25 expression stimulates glucose metabolism. At pathological conditions TPPP/p25 is localized in inclusion bodies in multiple system atrophy, it tightly co-localizes with α-synuclein, partially with tubulin and not with vimentin. The previous and the present studies obtained with immunohistochemistry with pathological human brain tissues rendered it possible to classify among pathological inclusions on the basis of immunolabelling of TPPP/p25, and suggest this protein to be a potential linkage between Parkinson's and Alzheimer's diseases.

Keywords: Intrinsically unstructured proteins; Energy state; Neurodegeneration

1. Introduction

Protein folding is required for conversion of linear polymer amino acids to stable 3D structure that comprises a functional protein molecule. Most cellular proteins are folded into a defined conformation, however, as it was recently discovered, there is a large group of natively unfolded proteins denoted as intrinsically unstructured proteins (IUPs) (Dunker et al., 2001). These unfolded proteins inappropriately exposing hydrophobic surface can initiate aberrant protein–protein interactions which result in the formation of protein aggregates; these multistep processes lead to the development of neurodegeneration. It was commonly observed in several neurological disorders defined histologically by the presence of specific inclusion bodies (Johnston et al., 1998).

α-Synuclein (Weinreb et al., 1996), a member of the synuclein family, proteins that are abundant in the brain, is an unfolded protein involved in neurodegenerative diseases. α-Synucleinopathies include so-called Lewy body diseases, like Parkinson's disease (PD) and diffuse Lewy body disease (DLBD), furthermore multiple system atrophy (MSA). All are associated with filamentous inclusions, mainly neuronal in PD and DLBD and predominantly oligodendroglial in MSA. Assembly of α-synuclein into filaments is a nucleation-dependent process accompanied by the transition

* Corresponding author. Tel.: +36 1 2793129; fax: +36 1 4665465.
E-mail address: ovadi@enzim.hu (J. Ovádi).
[1] These authors contributed equally to the work.

0248-4900/$ - see front matter © 2004 Elsevier SAS. All rights reserved.
doi:10.1016/j.biolcel.2004.08.002

from random-coil conformation to a β-pleated sheet (Serpell et al., 2000). In fact, intracellular (α-synuclein, hyperphosphorylated tau) or extracellular (β-amyloid) deposits of aggregated proteins with β-sheet structure characterize neurodegenerative diseases. The potential involvement of some glycolytic enzymes in the neurodegeneration is based upon the demonstration that they bind to proteins important to the pathogenesis of several neuronal disorders (Ovádi et al., 2004 and references therein). For example, glyceraldehyde-3-phosphate dehydrogenase (GAPD), a multifunctional glycolytic enzyme, binds to α-synuclein, huntingtin or β-amyloid precursor protein, which may result in structural and/or functional alterations; GAPD co-localizes with α-synuclein in Lewy body in PD cells (Schulze et al., 1993; Mazzola and Sirover, 2002; Lindersson et al., 2004). Evaluation of factors contributing to the ordered assembly of α-synuclein is essential to understand the pathogenesis of these common neurodegenerative diseases, thus, their role in physiological and pathological processes need to be identified and characterized at different levels.

TPPP/p25 was independently identified as a brain-specific protein occurring mainly in oligodendrocytes and in the neuropil (p25α) (Takahashi et al., 1991,1993) and as a tubulin-binding protein isolated from bovine brain (Hlavanda et al., 2002). The primary sequence of this protein is completely different from any other proteins available in the data banks. It promotes the polymerization of tubulin at substoichometric concentration (tubulin polymerization promoting protein, TPPP) into double walled tubules and polymorphic aggregates, or bundles paclitaxel-stabilized microtubules (Hlavanda et al., 2002). Injection of bovine TPPP/p25 into dividing *Drosophila* embryos expressing tubulin-GFP fusion protein reveals that TPPP/p25 inhibits mitotic spindle assembly and GTP counteracts TPPP/p25 (Tirián et al., 2003). In a recent study, we have demonstrated by immunohistochemistry and confocal microscopy that TPPP/p25 is enriched in filamentous α-synuclein bearing Lewy bodies of PD and DLBD, as well as glial inclusions of MSA; however, TPPP/p25 is not associated with abnormally phosphorylated tau in various intracellular aggregates of Pick's disease, progressive supranuclear palsy, and corticobasal degeneration (Kovács et al., 2004).

In this paper, we further characterized the structural and pathological properties of this new brain-specific protein, and these data are compared with that of other unfolded proteins involved in neurodegeneration. The following issues are specifically considered: (i) characterization of the structure of TPPP/p25: predictions and experiments; (ii) the effect of expression of TPPP/p25 on the energy production of neuroblastoma cells: cellular, biochemical and computation studies; (iii) localization of TPPP/p25 in pathological human brain tissues: evaluation of its distinct character in neurological diseases.

2. Results and discussion

2.1. Unfolded structures

The term "intrinsically unstructured" or "intrinsically disordered" designates proteins or protein domains that are unstructured in vitro under physiological conditions in absence of a binding partner (Dunker et al., 2001; Uversky, 2002; Tompa, 2002). There are common sequence features of the proteins belonging to this family, which make them distinct from globular proteins. They are generally depleted in the so-called "order-promoting" amino acids: W, C, F, I, Y, L, N, (V) and enriched in "disorder-promoting" amino acids: Q, S, P, E, K, (A, R, G) (Dunker et al., 2001; Tompa, 2002). Here, we explore how the properties of TPPP/p25 correspond to these criteria. Fig. 1A shows, TPPP/p25 is depleted in all "order-promoting" amino acids and enriched in most "disorder-promoting" residues.

A neural network-based algorithm, PONDR®, has been developed to search naturally disordered regions of proteins (Li et al., 1999; Romero et al., 2001). This method renders possible prediction of long disordered and ordered regions (>40 amino acids) of proteins with very good confidence. Using this predictor, we found that TPPP/p25 (both human and bovine) contains one long disordered region, namely the

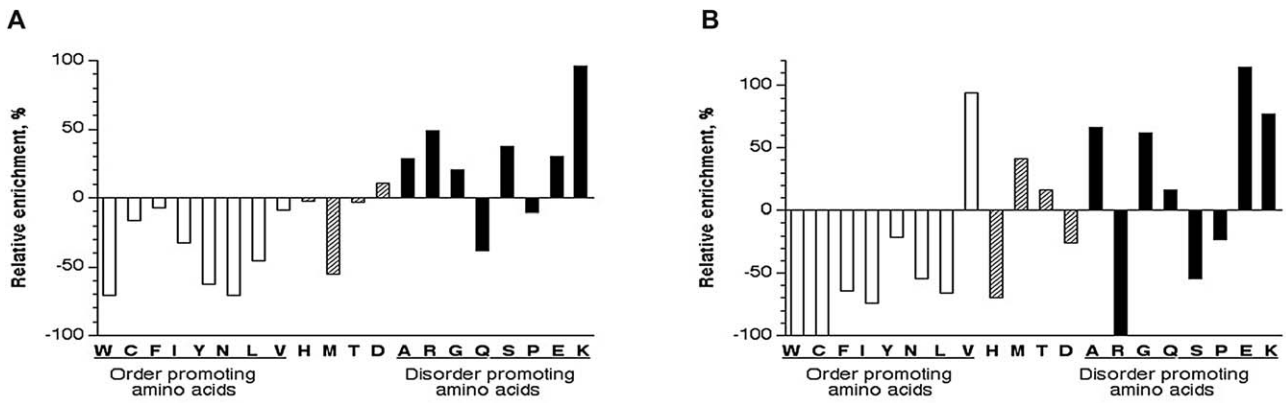

Fig. 1. Amino acid composition profiles of TPPP/p25 (A) and α-synuclein (B): deviation from globular proteins. Order-promoting and disorder-promoting amino acids are indicated by empty and black bars, respectively. Ambivalent amino acids are represented by striped bars.

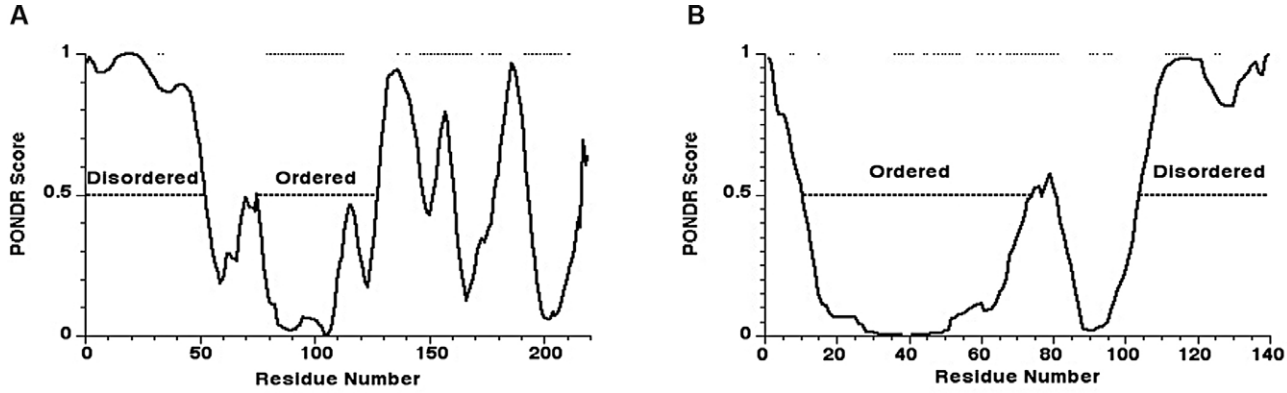

Fig. 2. PONDR® predictions of structural disorder of TPPP/p25 (A) and α-synuclein (B). Disorder prediction values (PONDR scores) for a given residue are plotted against the residue number. The significance threshold, above which residues are considered to be disordered set to 0.5, is shown. Long ordered and disordered regions are denoted by dotted lines. Stabilization centre residues predicted by the SCPRED program are labelled by spots on the top of the figure.

N-terminal part (the first 52 and 54 residues, respectively) (Fig. 2A). In the middle part of the protein an ordered region of similar length (52 residues) was predicted, while the C-terminal part contains a pattern of alternating ordered and disordered short sections. The overall percent of disordered residues was 46–47%. Since PONDR® tends to under predict disordered regions (Dunker et al., 2002b), we can suppose that at least half of the protein possesses disordered structure.

We used another neural network based program (SCPRED) for prediction of amino acid residues involved in strong long-range interactions, denoted as "stabilization centres" (Dosztányi et al., 1997). The program can help in prediction of the folding class of a protein with unknown structure. We found no stabilization centres in the first 77 amino acid of bovine TPPP/p25 and only two of them in the human form (Fig. 2A). Stabilization centre residues are supposed to be responsible for the prevention of the decay of the folded structure thus lack of them are indicative for the unfolded structure of the N-terminal end of TPPP/p25. On the contrary, most of the stabilization centres were predicted to be in the middle, ordered region.

The N-terminal part of TPPP/p25 is of special of interest since this part is missing in the shorter analogues of TPPP/p25 encoded by two distinct genes in mammals (Tirián et al., 2003). A phosphorylation site motif (TPPKSP) within this segment is present in microtubule associated tau protein as well. Tau is also an IUP, hyperphosphorylation of which plays an important role in the pathomechanism of Alzheimer's disease (AD), and this phosphorylation site motif is also located in its unstructured part. This sequence is a cdk5 phosphorylation site in tau, and it could be phosphorylated by cdk5 in TPPP/p25 in vitro (Takahashi et al., 1991). Since the action of IUPs is often modulated by phosphorylation (Dunker et al., 2002a; Tompa, 2002), one can speculate that the phosphorylation of this site in TPPP/p25 has also physiological/pathological significance.

α-Synuclein is considered as one of the prototypes of IUPs supported by both experimental (Weinreb et al., 1996) and our prediction data (cf. Table 1). Its long disordered segment, in contrast to TPPP/p25, is located at the C-terminal end (the residues 104–140 according to the PONDR® prediction) (Fig. 2B). Amino acid composition of α-synuclein is characteristic for IUPs (for example, complete lack of Trp and Cys, very high Glu content), apart from the lack of Arg and the extreme high Val content (Fig. 1B). However, only one of the 19 Val residues can be found in the C-terminal part (97–140), where the majority of the residues responsible for unfolded state, for example, all of the Pro, are clustered. On the contrary, the isolated N-terminal region (1–96) was predicted to fold (Uversky et al., 2001). Interestingly, in an alternatively spliced form of α-synuclein, the 103–140 amino acids are removed (Uéda et al., 1994).

Fluorescence measurements were carried out to establish the folding state of TPPP/p25 (Fig. 3). The maximum of the spectrum of the intrinsic fluorescence is at 350 nm which is significantly higher as compared to a globular protein (325 nm). Triosephosphate isomerase (TPI), a well-characterised globular protein, was used as a control to monitor the shift of the maximum of the emission spectrum by elevation of the temperature due to unfolding of this protein (Fig. 3, insert). From 5 to 55 °C the maximum is unchanged, it appears at 325 nm. It reaches 350 nm only at 75 °C which corresponds to the value measured with TPPP/p25 at 25 °C. This finding suggests that TPPP/p25 exists in an unfolded state at 25 °C, and reinforces our previous finding obtained by NMR (Kovács et al., 2004).

Table 1, which summarizes our prediction and experimental data for TPPP/p25 as compared to that of α-synuclein, shows that the characteristics of TPPP/p25 correspond to that of an IUP. An interesting feature of IUPs is that many of them contain sequence tandem repeats (Tompa, 2003). For instance, tau proteins contain 3–5 repeat units of 31 amino acids, which can be found in their tubulin binding region. α-Synuclein has five homologous repeat units of 11 amino acids, which was suggested to be involved its interaction with lipid membranes and synaptosomes (Perrin et al., 2000). TPPP/p25 possesses no repetitive sequence motifs, however, it has a motif (163–189 amino acids) homologous (43%) to the tau tubulin binding consensus sequence.

Table 1
Data revealing the unstructured nature of human α-synuclein and TPPP/p25

	α-Synuclein [a]	TPPP/p25
Number of amino acids	140	219
MW	14460 Da	23.472 Da
PI	6.1	9.5
Net charge	–10	+10
Heat stable	Yes	Yes [b]
High apparent MW by SDS-PAGE	Yes	No [b]
High apparent MW by gel filtration	Yes	No data
Slow sedimentation indicating elongated structure	Yes	No data
Lack of significant secondary structure detected by	Far UV CD	Far UV CD [b]
	(2% α-helix)	(4% α-helix) [b]
	FTIR (broad amid I)	NMR (broad amid I) [c]
		Fluorescence spectrum [d]
Addition of TFE increase the α-helix	2–39%	4–43% [d]
Amino acid composition characteristic for IUPs	Yes [d]	Yes [d]
Low aromaticity	4.29% [d]	5.48% [d]
Repeat expansions	5 × 11	No [d]
Predicted long disordered region	104–140 (C-terminus) [d]	1–52(N-terminus) [d]

[a] Data for α-synuclein from Weinreb et al. (1996).
[b] Hlavanda et al. (2002).
[c] Kovács et al. (2004).
[d] This study.

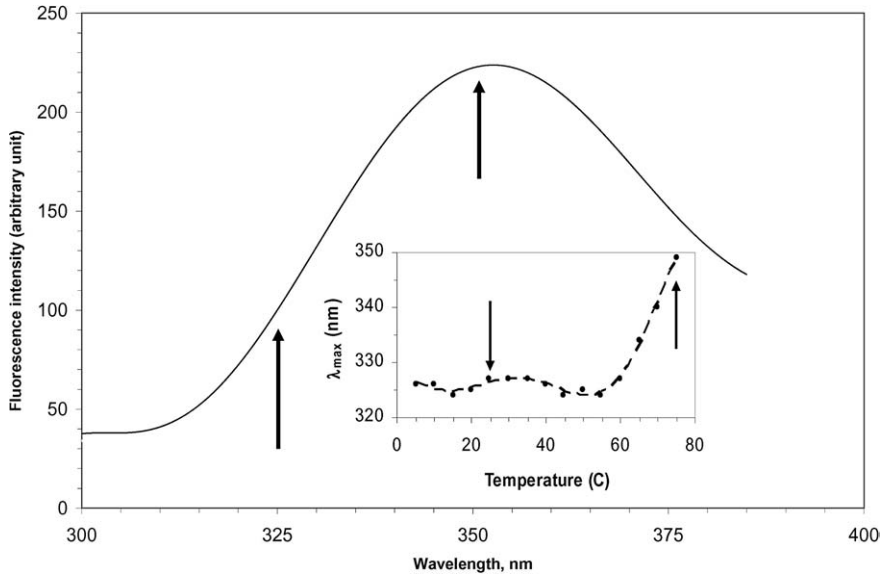

Fig. 3. Intrinsic fluorescence emission spectrum of TPPP/p25 at 25 °C. The insert shows the change of maximum position of the emission spectrum of TPI as a function of temperature. Excitation wavelength was 280 nm, concentration of proteins were 50 μg/ml.

A characteristic feature of many of IUPs is that their structures can be transiently folded (ordered) due to their binding to targets. Experimental data show that the majority of IUPs folds upon binding to their physiological partners (Dyson and Wright, 2002). The inherent secondary structure preferences of IUPs are characterized by a tendency to form α-helixes rather then β-sheets (Fuxreiter et al., 2004). For instance, on binding to lipid membranes or detergent micelles, α-synuclein undergoes a structural transition to an α-helical conformation (Goedert, 2001).

The solvent 2,2,2-trifluoroethanol (TFE) mimics the hydrophobic environment experienced by proteins in protein–protein interactions and is therefore widely used as a probe to discover regions that have a propensity to undergo an induced folding (Hua et al., 1998). In the case of α-synuclein a significant increase in the α-helix content could be induced (cf. Table 1). However, a C-terminal peptide (96–125), which was synthesized, showed little tendency toward α-helix formation (2–6%), even in the presence of 50% TFE (Weinreb et al., 1996).

Here, we studied the effect of TFE on the structural alteration of TPPP/p25. Circular dichroism (CD) spectra of TPPP/p25 show an increased α-helicity (4–43%) upon the addition of TFE, as indicated by the characteristic minimum at 222 nm (Fig. 4). The use of TFE reveals an α-helix forming potential of this natively unfolded protein. This result sug-

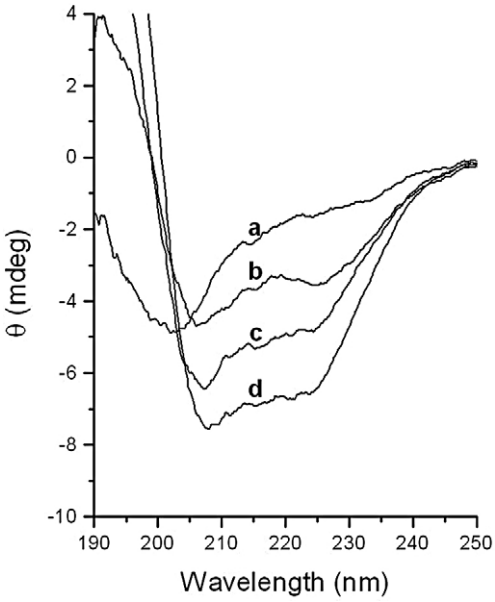

Fig. 4. Effect of TFE on the CD spectrum of TPPP/p25 isolated from bovine brain. a: 0%; b: 25%; c: 50%; d: 85% TFE. The concentration of TPPP/p25 was 2 μM.

gests that TPPP/p25 may undergo on significant unfolded–folded transition when interacts with its physiological partner(s).

2.2. Effect of TPPP/p25 on the energy state of the cells

Interactions of some key glycolytic enzymes with unfolded proteins which are the major players of the development of neurodegenerative diseases (PD, AD) have been demonstrated (Ovádi et al., 2004 and references therein). The functional consequences of these aberrant protein–protein interactions can affect the energy metabolism in brain tissue. The binding of phosphofructokinase (PFK) to β-amyloid inhibits the kinase activity (Meier-Ruge and Bertoni-Freddari, 1997 and references therein). The inhibition of PFK decreases glucose turnover and subsequently the oxidative phosphorylation. Reduction of GAPD activity was demonstrated in Huntington's disease and AD cells (Mazzola and Sirover, 2001). GAPD was identified as α-synuclein filament-binding protein in search for brain proteins that selectively bind to aggregated α-synuclein (Lindersson et al., 2004). This fact is of special interest since we recently showed that TPPP/p25 is enriched in inclusions specific for α-synucleinopathies (Kovács et al., 2004). The pathomechanism and significance of these processes is yet unclear. However, it is likely that the decline of glucose turnover can accelerate the progression of neurodegeneration, since the glucose is the major energy source in brain.

To examine the effect of the expression of TPPP/p25 on the energy state and glucose metabolism, neuroblastoma (SK-N-MC) cells were transfected with pEGFP-TPPP/p25 construct. Stable clones were selected expressing the fusion protein as described in Section 3, and one of these lines (K4) was used for further examinations. The overall view of these cells is shown in Fig. 5A obtained by epifluorescent microscopy. The EGFP-TPPP/p25 does not distribute homogeneously within the cytoplasm of cells but it appears to be aligned along filament network. The filament involved

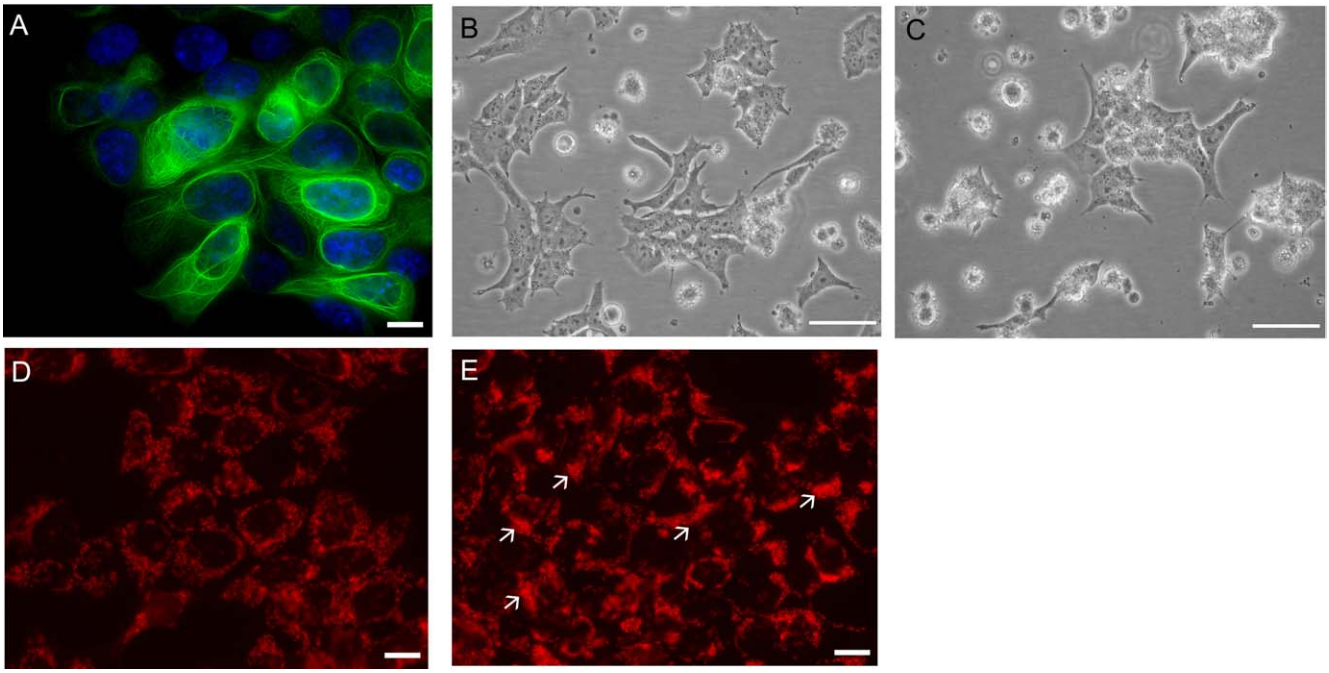

Fig. 5. Microscopic study of K4 cells. (A) Fluorescence image of K4 cells expressing EGFP-TPPP/p25 fusion protein; nuclei are stained with DAPI. Magnification 1000x; bar, 10 μm. (B and C) Phase-contrast images of SK-N-MC (mother) cells (B) and K4 cells (C) at low density. Morphologically the two cell lines look similar. Magnification: 500x; bars, 20 μm. (D and E) Fluorescence images of living SK-N-MC (D) and K4 cells (E) treated with TMRE. TPPP/p25 expressing (K4) cells show enhanced uptake (more intense red signal; see the arrows) of TMRE (E) as compared with the SK-N-MC cells (D). Magnification 400x, bars, 25 μm.

Table 2
Activity of glycolytic enzymes in the homogenates of the control and of K4 cells. The preparation of cell homogenates from SK-M-NC (control) and K4 cells and the activity measurements were carried out as described in Section 3. The data and standard deviations are from three independent measurements

	Activities in cell homogenate U/g protein	
Enzyme	Control	K4
HK	10.0 ± 0.1	12.0 ± 0.3
Glucose-6-phosphate isomerase	28.9 ± 2	35.9 ± 1
PFK	60.5 ± 5	102 ± 25
Aldolase	197 ± 60	199 ± 30
TPI	1880 ± 185	2390 ±240
GAPD	490 ± 10	552 ± 20

in the co-localization is most probably the microtubular network, which extensively binds TPPP/p25 as we have demonstrated in vitro (Hlavanda et al., 2002) and in vivo in *Drosophila* embryo (Tirián et al., 2003). The phase-contrast microscopic images of K4 and control cells show similar morphology (Fig. 5B,C).

Mitochondrial membrane potency, which regulates the production of high-energy phosphate, is an important parameter determining the fate of the cells (Iijima et al., 2003). Therefore, a fluorescent dye, tetramethylrhodamine ethyl ester (TMRE), characteristic for the hyperpolarized membranes due to the extensive TMRE accumulation (Collins and Bootman, 2003), was used to monitor the membrane-related energy-producing system in the control and K4 cells. The comparison of the fluorescence images of SK-N-MC and K4 cells loaded with TMRE (Fig. 5D,E) show that in some cases (indicated by arrow in Fig. 5E) higher fluorescence intensity can be visualized in the case of the TPPP/p25 expressing cells. These data suggest that the TPPP/p25 does not damage, rather stimulates the production of the intracellular high-energy phosphate at least as long as the morphology of the TPPP/p25 expressing cells do not change.

To obtain quantitative data for the effect of TPPP/p25 on the cellular ATP level, a key parameter of the energy state, the ATP concentration was determined in the control and K4 cells. We have found that the ATP concentration is 1.5-fold higher in the extract of the K4 clone as compared to that of the control cells (26.6 ± 3.0 μM/g protein and 17.2 ± 1.8 μM/g protein, respectively). These data obtained from three parallel measurements are in concert with that deduced from the cellular studies.

Next, we searched for the biochemical base of the enhanced ATP level by analyzing the activities of the individual glycolytic enzymes, which have been suggested to be involved in neurodegeneration (see Section 1). The enzymatic activities were determined in the cell homogenates of the control and K4 cells. Table 2 summarizes the activities of the glycolytic enzymes of the upper part of this pathway. Except aldolase, the activities of other enzymes are significantly higher in the case of K4 cells than in the control. In order to test the consequence of the TPPP/p25-induced enzyme activities at system level, flux measurements were carried out

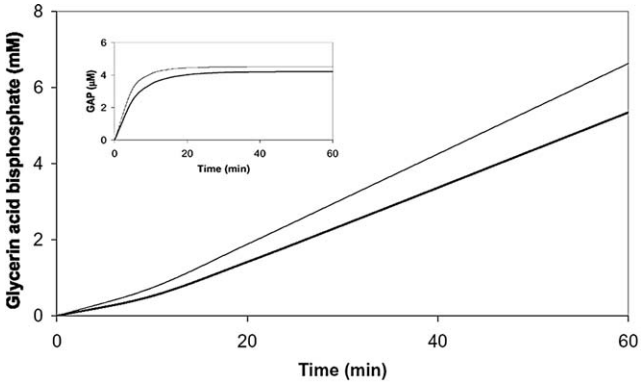

Fig. 6. Computed fluxes of glucose conversion to glycerine acid bisphosphate in homogenates of control and K4 cells. Solid line: clone K4 expressing TPPP/p25; bold line: control. Insert shows the change of concentration of the last intermediate, GAP, in time indicating that the system can reach the steady-state in 20 min at 5 mg/ml protein concentration. Mathematica 4.2 was used for computation.

with the cell homogenates. However, the determination of the steady-state rates for the conversion of glucose into glycerine acid bisphosphate by the six consecutive reactions was impossible due to the inactivation of HK, PFK and GAPD under test tube conditions. Thus, the flux of the consecutive reactions was computed by using the activity of the individual enzymes determined from the initial rates to overcome the inactivation of the enzymes. This approach rendered it possible to predict the fluxes of both control and K4 cells even at quasi physiological concentrations of the enzymes.

The fluxes were computed by using a mathematical model with kinetic parameters and rate equations of individual enzymatic reactions presented in Section 3.13. Fig. 6 shows the progress curves of glucose conversion and the time dependent changes of the concentration of the last intermediate, glyceraldehyde-3-phosphate (GAP), in both cell homogenates. As expected from the data of Table 2, the rate of glucose consumption is stimulated by the presence of TPPP/p25. The cellular, biochemical and computation results suggest that the expression of the unfolded TPPP/p25 in K4 cells can be tolerated by responding with extensive energy production.

2.3. TPPP/p25 accumulation in pathological human brain

Characterization of interactions of proteins and energy state in neurons and glia is crucial for understanding the pathogenesis of misfolding diseases. In neurodegenerative disorders abundant proteins are associated with different inclusions. However, the majority, including tubulin (Fig. 6 and Table 3), can be differentiated from α-synuclein or hyperphosphorylated tau on the basis that they immunolabel much fewer pathological cellular inclusions, or their aggregation or genetic linkage cannot be proved. α-Synuclein binds to tau (Jensen et al., 1999), MAP1B (Jensen et al., 2000), and to free unpolymerized tubulin α and β (Payton et al., 2001), as well as to microtubules (Alim et al., 2002). Tubulin may be able to initiate the polymerization of

Table 3
Comparison of immunolabelling for β-amyloid, ubiquitin, hyperphosphorylated tau, β-tubulin, TPPP/p25, α-synuclein and SMI-31. Black color indicates immunoreactivity, gray color indicates occasional immunoreactivity, white color indicates lack of immunoreactivity, while striped box indicates dot-like immunoreactivity. Occurrence of β-amyloid, ubiquitin, tau, α-synuclein and SMI-31 (reacts with phosphorylated epitope on neurofilament H and immunolabels granules of GVD) in the inclusions in relation to TPPP/p25 were demonstrated in pathological human brain tissues as described in Kovács et al. (2004)

	Parkinson's disease		Unspecific + Aging		Alzheimer's disease		
Pathology / Antibody	Lewy body	Cytoplasm body	GVD	Perisomatic granule	Pre-tangle	NFT	Amyloid plaque
β-amyloid							
Ubiquitin							
SMI-31							
Tau							
Tubulin							
α-synuclein							
TPPP/p25							

α-synuclein resulting in the formation of fibrils (Alim et al., 2002), thus, factors which affect microtubule assembly/disassembly are expected to be potential regulators of α-synuclein aggregation. TPPP/p25 physically interacts with tubulin and microtubules and promotes the formation of abnormal microtubule assemblies (Hlavanda et al., 2002). The observations that the major cellular target of TPPP/p25 is the microtubular system (Hlavanda et al., 2002; Tirián et al., 2003), suggest that TPPP/p25 may be actively involved in tubulin-induced α-synuclein fibril formation.

The spectrum of structures immunolabelled by anti-TPPP/p25 clearly overlaps with that of α-synuclein immunoreactive Lewy bodies and other neuronal and glial cytoplasmic aggregates in PD, DLBD, and MSA (Kovács et al., 2004). Here, we show that TPPP/p25 immunolabels glial cytoplasmic Papp-Lantos inclusions in a similar manner as does α-synuclein, while β-tubulin shows only partial immunoreactivity and vimentin is lacking (Fig. 7). In addition, it is related to early but not compact tau inclusions in AD and to granules of granulovacuolar degeneration (GVD). GVD is a non-disease-specific pathological change, thought to be the end stage of a sequestration process of degraded cellular components, including those related to the microtubular system, and proteins. It is mainly restricted to the hippocampus and mostly associated with ageing with an increased frequency in AD and Pick's disease. Interestingly, biochemically clearly distinguishable tauopathies like progressive supranuclear palsy, corticobasal degeneration, or Pick's disease lack TPPP/p25 immunopositivity in any kind of disease-specific intracellular hyperphosphorylated tau immunoreactive inclusions. This is in contrast with that observed with ubiquitin, which immunolabels specifically the majority of intra-, and extracellular deposits of aggregated proteins (Table 3). Hence, the role of TPPP/p25 is mainly restricted to the aggregation process of α-synuclein. The fact that tubulin is apparently able to initiate the seeding process of α-synuclein fibril formation, furthermore, that it is a component of Lewy bodies in PD and glial inclusions in MSA emphasizes the pathogenic role of factors, like TPPP/p25, able to disrupt the tubulin machinery (Fig. 7). Theoretically, genetic or epigenetic upregulation of TPPP/p25, as a putative microtubule disrupting element, as shown by our in vitro electron microscopic observation (Hlavanda et al., 2002), might be an early step in the complex pathogenesis of α-synucleinopathies.

To establish the relation of TPPP/p25 to the main protein components in PD, AD, and certain age-related pathological alterations like GVD, we summarized the present and previous data from our and other laboratories (Kovács et al., 2004 and references therein) for the spectrum of immunolabelling with α-synuclein, TPPP/p25, tubulin, hyperphosphorylated tau, and β-amyloid (Table 3). This demonstrates the specificity of TPPP/p25 for α-synuclein aggregates as compared with other markers; furthermore, it supports the notion that TPPP/p25 is related to the tubulin machinery by the appearance of immunoreactivity in the granules of GVD. The combined data set clearly shows that TPPP/p25 having a high

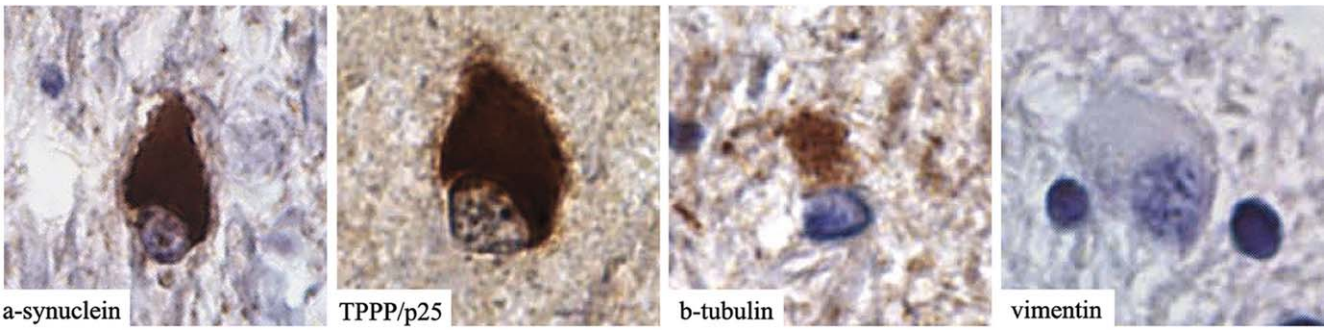

Fig. 7. Immunohistochemistry of human pathological brain tissue for α-synuclein, TPPP/p25, β-tubulin, and vimentin in MSA. Formalin fixed paraffin-embedded tissue from patients were used for immunohistochemical studies as described in Section 3. Specific antibody raised against to the 186–200 peptide of TPPP/25 was produced as described (Kovács et al., 2004). TPPP/p25 immunolabels glial cytoplasmic Papp-Lantos inclusions in a similar manner as done in α-synuclein, while β-tubulin does not show immunoreactivity in the full extent of the inclusions, and vimentin immunopositivity is completely lacking.

specificity to α-synuclein inclusions is a novel marker of synucleinopathies, and allows one to distinguish between synucleinopathies and tauopathies. An additional important issue can be deduced from the presence in early neurofibrillary tangle formation, that TPPP/p25 might be a linkage protein between AD and PD answering an unsolved question about overlapping or synergistic pathologies (Kurosinski et al., 2002).

In neurodegenerative diseases the connection between the accumulation of misfolded/unfolded protein aggregates, energy state/metabolism and phenotype of diseases is not completely understood. Identification of new proteins contributes extensively to insight into the "unfolding pathway" in disease pathogenesis, and to discover novel targets such as TPPP/p25 for therapeutic interventions in neurodegenerative diseases.

3. Materials and methods

3.1. Materials

Aldolase, glycerol-3-phosphate dehydrogenase, glycerol-3-phosphate dehydrogenase/TPI from rabbit muscle, glucose-6-phosphate dehydrogenase from yeast, ATP, fructose, fructose 1,6-diphosphate, fructose-6-phosphate, glucose, glucose-6-phosphate, GAP, NAD, NADH, NADP were purchased from Sigma Chemical (St. Louis, MO). All other chemicals were reagent-grade commercial preparations. Milli-Q (Millipore, Bedford, MA) ultrapure water was used for preparing the solutions.

TPPP/p25 was purified from bovine brain as described in Hlavanda et al. (2002).

3.2. Amino acid composition analysis

The average sequence composition of globular proteins was taken from Tompa (2002). If the average composition of an amino acid, X, in globular proteins is CG_X, and the composition of X in a protein P is CP_X, deviation from the composition of X in globular proteins was defined for P as $(CP_X - CG_X)/CG_X$.

3.3. Prediction of unstructured regions and stabilization centres

Sequences were submitted to the PONDR server (http://www.pondr.com) using the default integrated predictor VL-XT (Li et al., 1999; Romero et al., 2001). Access to PONDR® was provided by Molecular Kinetics (IUETC; Indianapolis, IN, USA; main@molekularkinetics.com) under the license from the WSU Research Foundation. PONDR® is copyright ©1999 by the WSU Research Foundation, all rights reserved. Sequences were analyzed by the SCPRED server (http://www.enzim.hu/scpred/), for prediction of "stabilization centres" (Dosztányi et al., 1997).

3.4. Fluorescence measurements

Fluorescence emission spectra were measured on a FluoroMax-3 spectrofluorometer (Jobin Yvon Inc., Longiumeau, France), using 1 cm thermostated cuvettes, and excitation and emission slits of 2 nm, in 20 mM phosphate buffer, pH 7.0 at, at excitation wavelength of 280 nm. Scanning was repeated three times, and the spectra were averaged.

3.5. Circular dichroism (CD) measurements

CD spectra were acquired with a Jasco J-720 spectropolarimeter (Tokyo, Japan) in the 190–280 nm wavelength range employing 0.1 cm thermostated cuvettes at 25 °C, in 10 mM phosphate buffer (pH 7.0). Spectra were corrected by subtracting the spectrum of the buffer from that of the sample. Scanning was repeated three times, and the spectra were averaged. The α-helical content was calculated from the measured ellipticity (Θ) value at 222 nm using the following equation (Chen et al., 1972):

$$\%\ \alpha\text{-helix} = \left(\left(\left| \Theta_{222} / (10ncl) \right| \right) - 2340 \right) / 303$$

where Θ is the ellipticity in millidegrees, n is the number of amino acid residues, c is the concentration in moles, and l is the path length of the cell in centimetres.

3.6. DNA manipulations of TPPP/p25 coding sequence

The coding region of human TPPP/p25 (Kovács et al., 2004) was fused to the C-terminus of EGFP by cloning TPPP/p25 ORF into pEGFP-C1 (Clontech) using the Bgl II and the *Eco*R I restriction sites (pEGFP-TPPP/p25).

3.7. Cell culture, transfections, and manipulations

SK-N-MC (ATCC, HTB-10) cells were grown in DME/F-12 medium supplemented with 10% FCS, 1 mM sodium pyruvate, 100 U/ml streptomycin, and 100 μg/ml penicillin (all Sigma) (complete medium) in humidified 37 °C incubator with 5% CO_2. Cells were transfected with pEGFP-TPPP/p25 by Fugene 6 reagent (Roche). Briefly, 1 μg plasmid and 3 μl Fugene 6 were mixed in 100 μl steril phosphate buffered saline, next the mixture stand at room temperature for 30 min. The whole mixture were added onto one 60-mm Petri dish containing the mother cell line at 50% confluency, and the transfected cells were grown for overnight. Selection of stable cells was done in the presence of 0.5 mg/ml G418 (Sigma). Surviving clones were subcloned. One of the stable clones was selected for further works contained the fluorescent fusion protein investigated by immunoblotting and fluorescence microscopy (referred as K4). Phase-contrast pictures of cultures were taken with Olympus CKX41 microscope equipped with Camedia C5050 digital camera. Olympus LCAch 40x objective was used. The cells were fixed with cold buffered ethanol and visualized by Leica DMLS (Leica Microsystems, Inc., Germany) epifluores-

cence microscope using C-PLAN 100x objective. The signal of EGFP was investigated by narrow band GFP filter set (Chroma Technology, Inc., USA). Spot 4.0.2 for Windows (Digital Instruments, Inc., USA) was used to acquire digital images. Images were post-processed with ImageJ (PC-based version of NIH Image).

3.8. Live cell imaging

For characterization of mitochondrial membrane polarization in live experiments, TMRE uptake was used (Collins and Bootman, 2003). Fluorescent images of live cells were recorded within 1 h. Temperated air flush (35 °C) was used to maintain temperature of the samples on the microscopic stage. TMRE fluorescence was detected with Leica filter set N2.1 (illumination of samples was kept minimally during the experimental period). Images were recorded on Leica DMLS microscope with C-PLAN 40x objective and processed as detailed above.

3.9. Immunohistochemistry

We obtained formalin fixed paraffin-embedded tissue blocks from the hippocampus of one neuropathologically confirmed AD case (79 years, female), mesencephalon of one PD case (67 years, female), and basal ganglia in one MSA case (48 years, female).

We used the polyclonal anti-TPPP/p25 antibody (Kovács et al., 2004) (1:200) after a pretreatment including 10 min microwave in citrate buffer and 1 min 88% formic acid. Further antibodies used were anti-ubiquitin (rabbit polyclonal, 1:200, Dako), anti-tau (mouse monoclonal AT8, 1:200, Innogenetics), anti-betaA4 (mouse monoclonal, 1:50, Dako), SMI-31 (mouse monoclonal, 1:5000, Sternberger Monoclonals Inc.), anti-α-synuclein (rat monoclonal, 1:20, Alexis Biochemicals), and anti-β-tubulin (mouse monoclonal, 1:1000, Sigma), anti-vimentin (mouse monoclonal, 1:200, Dako). As a secondary system we used the ChemMate™ and Envision™ detection kits (Dako) including diaminobenzidine as chromogenic substrate.

3.10. Preparation of cell homogenate

SK-N-MC or K4 cells were collected at 2000 g at 4 °C for 20 min, and then were diluted into 20 mM Tris–HCl buffer, pH 7.0, containing 1 mM ethylenediamine tetraacetic acid, 1 mM 1,4-dithioerythritol, 1 mM phenylmethanesulfonylfluoride and 1% Triton. The cells were then lysed by sonication with five short bursts of 5 s, followed by intervals of 30 s for cooling in ice and this homogenate was used for enzymatic measurements. The total protein concentration was determined by the method of Bradford (1976).

3.11. Enzymatic assays

The experiments were carried out in standard buffer (100 mM Tris, pH 8.0) at 37 °C by Cary100 spectrophotometer at 340 nm. Enzyme activities were determined according to Beutler et al. (1977). GAPD assay was carried out in standard buffer containing 5 mM arsenate, 4 mM NAD and 2 mM GAP as substrate. The ATP-level was determined in standard buffer containing 10 mM phosphate, 10 mM Mg^{2+}, 1 mM glucose, 1 mM NADP, and HK and glucose-6-phosphate dehydrogenase as auxiliary enzymes.

3.12. Simulation tools

All the numerical simulations were performed with Mathematica for Students (version 4.2) software package (Wolfram Research, http://www.wolfram.com).

3.13. Rate equations and kinetic parameters of the individual enzymatic reactions used for modelling

For the two major control enzymes, HK and PFK, Michaelis-Menten mechanisms were considered for the simulation of consecutive reactions, since: (i) no inhibition of HK by glucose-6-phosphate occurred in the presence of inorganic phosphate; (ii) substrate saturation of PFK is not sigmodial in cell extracts (Orosz et al., 2002). Mechanisms of the reactions catalysed by GPI, aldolase and TPI were taken from the model of Mulquiney and Kuchel (1999). In the case of GAPD Michaelis-Menten kinetics was assumed. Maximal rate (V_m) values, expressed in U/L, corresponded to 5 mg/ml total protein concentration were obtained from the experimentally determined initial rate of enzymatic reactions (see Table 2). Other kinetic parameters (K_m, K_i, K_e) were taken from the model of Mulquiney and Kuchel (1999) for all reactions apart from that of TPI which were experimentally determined.

Abbreviations: V_m: maximal rate, K_m: Michaelis-Menten constant, K_i: inhibitory constant, K_e: equilibrium constant, Glu: glucose, G6P: glucose-6-phosphate, F6P: fructose-6-phosphate, FDP: fructose1,6-diphosphate, DHAP: dihydroxyacetone phosphate, t: time.

(1) Hexokinase HK EC 2.7.1.1

$$v^{HK} = \frac{v_m^{HK} \times Glu[t]}{K_m^{HK} + Glu[t]};\ K_m^{HK} = 50\ \mu M$$

(2) Glucose-6-phosphate isomerase GPI EC 5.3.1.9

$$v^{GPI} = \frac{v_m^{GPI} \times \left[-\frac{F6P[t]}{K_e^{GPI}} + G6P[t] \right]}{K_m^{GPI} \times \left[1 + \frac{F6P[t]}{K_m^{GPI1}} + \frac{G6P[t]}{K_m^{GPI}} \right]}$$

$$K_m^{GPI} = 200\ \mu M;\ K_e^{GPI} = 0.329;\ K_m^{GPI1} = 80\ \mu M$$

(3) Phosphofructokinase PFK EC 2.7.1.11

$$v^{PFK} = \frac{v_m^{PFK} \times F6P[t]}{K_m^{PFK} + F6P[t]};\ K_m^{PFK} = 100\ \mu M$$

(4) Aldolase Ald EC 4.1.2.13

$$v^{\mathrm{ALD}} = \frac{v_{\mathrm{m}}^{\mathrm{ALD}} \times \left[\frac{\mathrm{FDP}[t]}{K_{\mathrm{m}}^{\mathrm{FDP}}} - \frac{\mathrm{DHAP}[t] \times \mathrm{GAP}[t]}{K_{\mathrm{e}}^{\mathrm{ALD}} \times K_{\mathrm{i}}^{\mathrm{DHAP}} \times K_{\mathrm{m}}^{\mathrm{GAP}}} \right]}{1 + \frac{\mathrm{DHAP}[t]}{K_{\mathrm{i}}^{\mathrm{DHAP}}} + \frac{\mathrm{FDP}[t]}{K_{\mathrm{M}}^{\mathrm{FDP}}} + \frac{K_{\mathrm{m}}^{\mathrm{DHAP}} \times \mathrm{GAP}[t]}{K_{\mathrm{i}}^{\mathrm{DHAP}} \times K_{\mathrm{m}}^{\mathrm{GAP}}} + \frac{\mathrm{DHAP}[t] \times \mathrm{GAP}[t]}{K_{\mathrm{i}}^{\mathrm{DHAP}} \times K_{\mathrm{m}}^{\mathrm{GAP}}} + \frac{K_{\mathrm{m}}^{\mathrm{DHAP}} \times \mathrm{FDP}[t] \times \mathrm{GAP}[t]}{K_{\mathrm{i}}^{\mathrm{DHAP}} \times K_{\mathrm{m}}^{\mathrm{FDP}} \times K_{\mathrm{m}}^{\mathrm{GAP}}}}$$

$K_{\mathrm{M}}^{\mathrm{FDP}} = 8\ \mu\mathrm{M}$; $K_{\mathrm{m}}^{\mathrm{GAP}} = 40\ \mu\mathrm{M}$; $K_{\mathrm{i}}^{\mathrm{DHAP}} = 10\ \mu\mathrm{M}$; $K_{\mathrm{m}}^{\mathrm{DHAP}} = 40\ \mu\mathrm{M}$; $K_{\mathrm{i}}^{\mathrm{FDP}} = 15\ \mu\mathrm{M}$; $K_{\mathrm{e}}^{\mathrm{ALD}} = 0.35$

(5) TPI EC 5.3.1.1

$$v^{\mathrm{TPI}} = \frac{v_{\mathrm{m}}^{\mathrm{TPI}} \times \left[-\frac{\mathrm{DHAP}[t]}{K_{\mathrm{e}}} + \mathrm{GAP}[t] \right]}{K_{\mathrm{m_I}}^{\mathrm{GAP}} \times \left[1 + \frac{\mathrm{DHAP}[t]}{K_{\mathrm{m_I}}^{\mathrm{DHAP}}} + \frac{\mathrm{GAP}[t]}{K_{\mathrm{m_I}}^{\mathrm{GAP}}} \right]}$$

$K_{\mathrm{m_I}}^{\mathrm{DHAP}} = 1300\ \mu\mathrm{M}$; $K_{\mathrm{e}} = 9$; $K_{\mathrm{m_I}}^{\mathrm{GAP}} = 650\ \mu\mathrm{M}$

(6) GAPD EC 1.2.1.12

$$v^{\mathrm{GAPD}} = \frac{v_{\mathrm{m}}^{\mathrm{GAPD}} \times \mathrm{GAP}[t]}{K_{\mathrm{m}}^{\mathrm{GAPD}} + \mathrm{GAP}[t]}$$

$K_{\mathrm{m}}^{\mathrm{GAPD}} = 100\ \mu\mathrm{M}$

Acknowledgements

This work was supported by Hungarian National Scientific Research Fund Grants OTKA T-046071 and B-044730 (to J. Ovádi) and T-035019 (F.O.), Hungarian Ministry of Education Grant OMFB-00701/2003 and Charles Simonyi fellowship (to J. Ovádi) and Bolyai fellowship (to K.G.G.).

References

Alim, M.A., Hossain, M.S., Arima, K., Takeda, K., Izumiyama, Y., Nakamura, M., et al., 2002. Tubulin seeds alpha-synuclein fibril formation. J. Biol. Chem. 277, 2112–2117.

Beutler, E., Blume, K.G., Kaplan, J.C., Löhr, G.W., Ramot, B., Valentine, W.N., 1977. International Committee for Standardization in Haematology: recommended methods for red-cell enzyme analysis. Br. J. Haematol. 35, 331–340.

Bradford, M.M., 1976. A rapid and sensitive method for the quantitation of microgram quantities of protein utilizing the principle of protein–dye binding. Anal. Biochem. 72, 248–254.

Chen, Y.-H., Yang, J.T., Martinez, H.M., 1972. Determination of the secondary structures of proteins by circular dichroism and optical rotatory dispersion. Biochemistry 11, 4120–4131.

Collins, T.J., Bootman, M.D., 2003. Mitochondria are morphologically heterogeneous within cells. J. Exp. Biol. 206 (12), 1993–2000.

Dosztányi, Z., Fiser, A., Simon, I., 1997. Stabilization centers in proteins: identification, characterization and predictions. J. Mol. Biol. 272, 597–612.

Dunker, A.K., Brown, C.J., Lawson, J.D., Iakoucheva, L.M., Obradovic, Z., 2002. Intrinsic disorder and protein function. Biochemistry 41, 6573–6582.

Dunker, A.K., Brown, C.J., Obradovic, Z., 2002. Identification and functions of usefully disordered proteins. Adv. Protein. Chem. 62, 25–49.

Dunker, A.K., Lawson, J.D., Brown, C.J., Williams, R.M., Romero, P., Oh, J.S., et al., 2001. Intrinsically disordered protein. J. Mol. Graph. Model. 19, 26–59.

Dyson, H.J., Wright, P.E., 2002. Coupling of folding and binding for unstructured proteins. Curr. Opin. Struct. Biol. 12, 54–60.

Fuxreiter, M., Simon, I., Friedrich, P., Tompa, P., 2004. Preformed structural elements feature in partner recognition by intrinsically unstructured proteins. J. Mol. Biol. 338, 1015–1026.

Goedert, M., 2001. Alpha-synuclein and neurodegerative diseases. Nat. Rev. Neurosci. 2, 492–501.

Hlavanda, E., Kovács, J., Oláh, J., Orosz, F., Medzihradszky, K.F., Ovádi, J., 2002. Brain-specific p25 protein binds to tubulin and microtubules and induces aberrant microtubule assemblies at substoichiometric concentrations. Biochemistry 41, 8657–8664.

Hua, Q.X., Jia, W.H., Bullock, B.P., Habener, J.F., Weiss, M.A., 1998. Transcriptional activator–coactivator recognition: nascent folding of a kinase-inducible transactivation domain predicts its structure on coactivator binding. Biochemistry 37, 5858–5866.

Iijima, T., Mishima, T., Akagawa, K., Iwao, Y., 2003. Mitochondrial hyperpolarization after transient oxygen–glucose deprivation and subsequent apoptosis in cultured rat hippocampal neurons. Brain Res. 993, 140–145.

Jensen, P.H., Hager, H., Nielsen, M.S., Hojrup, P., Gliemann, J., Jakes, R., 1999. Alpha-synuclein binds to Tau and stimulates the protein kinase A-catalyzed tau phosphorylation of serine residues 262 and 356. J. Biol. Chem. 274, 25481–25489.

Jensen, P.H., Islam, K., Kenney, J., Nielsen, M.S., Power, J., Gai, W.P., 2000. Microtubule-associated protein 1B is a component of cortical Lewy bodies and binds alpha-synuclein filaments. J. Biol. Chem. 275, 21500–21507.

Johnston, J.A., Ward, C.L., Kopito, R.R., 1998. Aggresomes: a cellular response to misfolded proteins. J. Cell Biol. 143, 1883–1898.

Kovács, G.G., László, L., Kovács, J., Jensen, P.H., Lindersson, E., Botond, G., et al., 2004. Natively unfolded tubulin polymerization promoting protein TPPP/p25 is a common marker of alpha-synucleinopathies. Neurobiol. Dis. 17, 157–162.

Kurosinski, P., Guggisberg, M., Götz, J., 2002. Alzheimer's and Parkinson's disease—overlapping or synergistic pathologies? Trends Mol. Med. 8, 3–5.

Li, X., Romero, P., Rani, M., Dunker, A.K., Obradovic, Z., 1999. Predicting protein disorder for N-, C-, and internal regions. Genome Inform. Ser. Workshop Genome Inform. 10, 30–40.

Lindersson, E., Beedholm, R., Hojrup, P., Moos, T., Gai, W., Hendil, K.B., Jensen, P.H., 2004. Proteasomal inhibition by alpha-synuclein filaments and oligomers. J. Biol. Chem. 279, 12924–12934.

Mazzola, J.L., Sirover, M.A., 2001. Reduction of glyceraldehyde-3-phosphate dehydrogenase activity in Alzheimer's disease and in Huntington's disease fibroblasts. J. Neurochem. 76, 442–449.

Mazzola, J.L., Sirover, M.A., 2002. Alteration of intracellular structure and function of glyceraldehyde-3-phosphate dehydrogenase: a common phenotype of neurodegenerative disorders? Neurotoxicology 23, 603–609.

Meier-Ruge, W.A., Bertoni-Freddari, C., 1997. Pathogenesis of decreased glucose turnover and oxidative phosphorylation in ischemic and trauma-induced dementia of the Alzheimer type. Ann. N. Y. Acad. Sci. 826, 229–241.

Mulquiney, P.J., Kuchel, P.W., 1999. Model of 2,3-bisphosphoglycerate metabolism in the human erythrocyte based on detailed enzyme kinetic equations: equations and parameter refinement. Biochem. J. 342, 581–596.

Orosz, F., Wágner, G., Ortega, F., Cascante, M., Ovádi, J., 2002. Glucose conversion by multiple pathways in brain extract: theoretical and experimental analysis. Biochem. Biophys. Res. Comm. 309, 792–797.

Ovádi, J., Orosz, F., Hollán, S., 2004. Functional aspects of cellular microcompartmentation in the development of neurodegeneration. Mutation induced aberrant protein–protein associations. Mol. Cell. Biochem. 256 (257), 83–93.

Payton, J.E., Perrin, R.J., Clayton, D.F., George, J.M., 2001. Protein–protein interactions of alpha-synuclein in brain homogenates and transfected cells. Brain Res. Mol. Brain Res. 95, 138–145.

Perrin, R.J., Woods, W.S., Clayton, D.F., George, J.M., 2000. Interaction of human alpha-synuclein and Parkinson's disease variants with phospholipids. Structural analysis using site-directed mutagenesis. J. Biol. Chem. 275, 34393–34398.

Romero, P., Obradovic, Z., Li, X., Garner, E.C., Brown, C.J., Dunker, A.K., 2001. Sequence complexity of disordered protein. Proteins 42, 38–48.

Schulze, H., Schuyler, A., Stuber, D., Dobeli, H., Langen, H., Huber, G., 1993. Rat brain glyceraldehyde-3-phosphate dehydrogenase interacts with the recombinant cytoplasmic domain of Alzheimer's β-amyloid precursor protein. J. Neurochem. 60, 1915–1922.

Serpell, L.C., Berriman, J., Jakes, R., Goedert, M., Crowther, R.A., 2000. Fiber diffraction of synthetic alpha-synuclein filaments show amyloid-like cross-beta conformation. Proc. Natl. Acad. Sci. USA 97, 4897–4902.

Takahashi, M., Tomizawa, K., Ishiguro, K., Sato, K., Omori, A., Sato, S., et al., 1991. A novel brain-specific 25 kDa protein (p25) is phosphorylated by a Ser/Thr-Pro kinase (TPK II) from tau protein kinase fractions. FEBS Lett. 289, 37–43.

Takahashi, M., Tomizawa, K., Fujita, S.C., Sato, K., Uchida, T., Imahori, K., 1993. A brain-specific protein p25 is localized and associated with oligodendrocytes, neuropil, and fiber-like structures of the CA3 hippocampal region in the rat brain. J. Neurochem. 60, 228–235.

Tirián, L., Hlavanda, E., Oláh, J., Horváth, I., Orosz, F., Szabó, B., et al., 2003. TPPP/p25 promotes tubulin assemblies and blocks mitotic spindle formation. Proc. Natl. Acad. Sci. USA 100, 13976–13981.

Tompa, P., 2002. Intrinsically unstructured proteins. Trends Biochem. Sci. 27, 527–533.

Tompa, P., 2003. Intrinsically unstructured proteins evolve by repeat expansion. Bioessays 25, 847–855.

Uéda, K., Saitoh, T., Mori, H., 1994. Tissue-dependent alternative splicing of mRNA for NACP, the precursor of non-A beta component of Alzheimer's disease amyloid. Biochem. Biophys. Res. Commun. 205, 1366–1372.

Uversky, V.N., 2002. Natively unfolded proteins: a point where biology waits for physics. Protein Sci. 11, 739–756.

Uversky, V.N., Gillespie, J.R., Fink, A.L., 2001. Why are "natively unfolded" proteins unstructured under physiologic conditions? Proteins 41, 315–427.

Weinreb, P.H., Zhen, W., Poon, A.W., Conway, K.A., Lansbury Jr., P.T., 1996. NACP, a protein implicated in Alzheimer's disease and learning, is natively unfolded. Biochemistry 35, 13709–13715.